Optics Communications 481 (2021) 126528

Contents lists available at ScienceDirect

Optics Communications

journal homepage: www.elsevier.com/locate/optcom

Tunable DFB laser diode based on high-order surface isolation grooves working at 905nm

Xia Liu [a,b], Yongyi Chen [a,c,*], Yugang Zeng [a,c,**], Li Qin [a,c], Liang Lei [a,c], Peng Jia [a], Hao Wu [a], Dezheng Ma [a,b], Chunkao Ruan [a,b], Yongqiang Ning [a], Lijun Wang [a,c]

[a] State Key Laboratory of Luminescence and Applications, Changchun Institute of Optics, Fine Mechanics and Physics, Chinese Academy of Sciences, Changchun, 130033, China

[b] Center of Materials Science and Optoelectronics Engineering, University of Chinese Academy of Sciences, Beijing, 100049, China

[c] Peng Cheng Laboratory No.2, Xingke 1st Street, Nanshan, Shenzhen, China

ARTICLE INFO

Keywords:
Tunable DFB laser
Laser diode

ABSTRACT

A widely tunable distributed feedback Bragg (DFB) laser diode based on surface isolation grooves has been produced by i-line lithography. Periodic p-electrodes on the mesas realize a single longitudinal mode output. The maximum continuous wave output power of the uncoated device was 145.3 mW/facet at 500 mA, and the maximum side-mode suppression ratio was over 37 dB. Experimentally, the laser diode could be tuned from 899.9 to 907.7 nm from 15 °C to 35 °C. The 3 dB linewidth was 920 MHz at 20 °C for an injected current of 300 mA. The method of fabricating the tunable DFB laser diode has great potential for many applications, such as in light detection and ranging (LiDAR) devices.

1. Introduction

Distributed feedback Bragg (DFB) laser diodes are important light sources in many applications in modern industry. The DFB laser diodes have the advantages of small size, stable wavelength characteristics, and ease of integration with other devices. They are used as pump sources in both fiber [1] and solid-state [2] lasers. Further, tunable DFB laser diodes are mainly used as light sources in optical modules [3] and many other micro-systems [4–6]. In particular, 905 nm wavelength DFB laser diodes are important components in photo-electrical sensing and photo-acoustic imaging [7–9] devices. Owing to the small attenuation in air and a good penetration effect, the 905 nm DFB laser diodes have a great potential for optical phase arrays in laser ranging [10,11], free-space line-of-sight optical communications, and light detection and ranging (LiDAR) in autonomous vehicles [12,13].

To the best of our knowledge, existing DFB lasers around a wavelength of 905 nm are all based on the index coupled effect [9,10]. Most of them are prepared by epitaxial regrowth methods, and such fabrication processes require complicated nanoscale lithography and etching techniques [14–17].

In our previous work [18–20], we already proposed some regrowth-free methods for fabricating gain-coupled DFB laser and taper laser diodes. For gain-guided lasers the spontaneous emission factor is taken to be large(as compared with that for index-guided lasers) and the gain profile is taken to be smooth and parabolic [21]. It is suitable for preparing tunable semiconductor lasers. The isolation grooves act as slot inside FP cavity can modulate the emission spectrum, The presence of surface isolation grooves inside the cavity of a semiconductor laser can have a very strong influence on the emission spectrum, It is helpful for the tunable DFB laser to improve the performance of single longitudinal mode [22–26].

In this paper, We combined surface gratings and periodic p-electrodes structures for fabricating our first 905 nm tunable DFB laser based on isolation grooves and smaller periodic electrode windows, Both gain-coupled mechanism and slot function are considered. By modulating the depth of the isolation grooves, we have recently demonstrated a tunable laser based on surface isolation grooves which completely relies on these grooves to provide necessary reflectivity for the laser operation independent of any etching facets [27]. Compared with the previous work results, the output power and the side-mode suppression ratio (SMSR) is improved, and the novel 905 nm tunable DFB laser can achieve greater tuning range. The central wavelength of this device can be tuned from 899.9 nm to 907.7 nm within a small temperature range. Compared with our previous periodic p-contacts gain-coupled DFB laser diodes, the device in proposed in this study has better thermal stability and wavelength modulation characteristics.

* Corresponding author at: State Key Laboratory of Luminescence and Applications, Changchun Institute of Optics, Fine Mechanics and Physics, Chinese Academy of Sciences, Changchun, 130033, China.

** Corresponding author.

E-mail addresses: chenyy@ciomp.ac.cn (Y. Chen), zengyg@ciomp.ac.cn (Y. Zeng).

https://doi.org/10.1016/j.optcom.2020.126528
Received 16 August 2020; Received in revised form 9 October 2020; Accepted 10 October 2020
Available online 13 October 2020

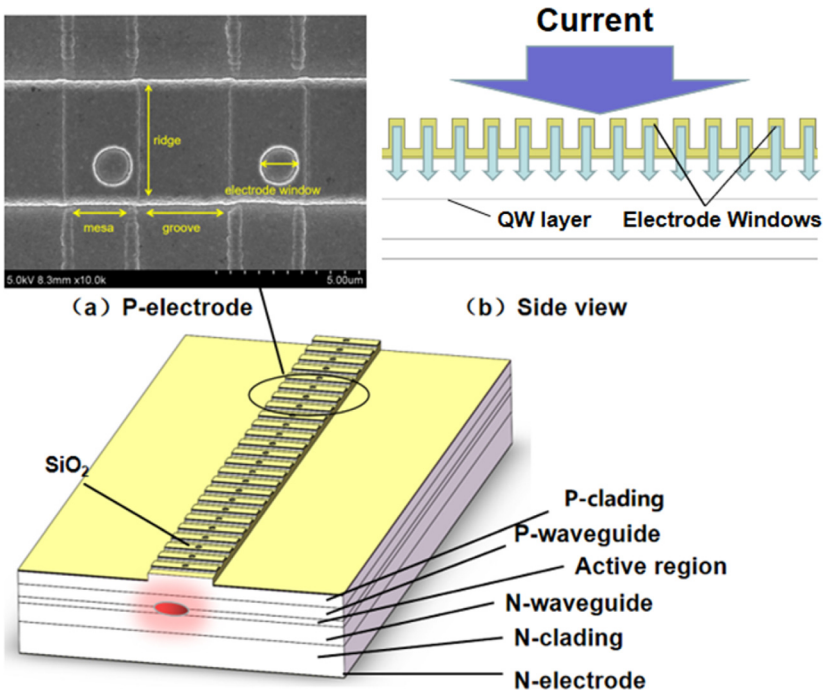

Fig. 1. Device Schematic (a) Scanning electron microscope image for the top of the device, (b) Side view of the device.

Table 1
Structure of the 905 nm chip.

Structure	Material	Thickness (μm)
1. Cap	P++ GaAs	0.15
2. P-clading	P+ $Al_xGa_{1-x}As(x = 0.05 - 0.45)$	1.05
Waveguide layers & Active region	$InGaAs/Al_xGa_{1-x}As$	2
4. N-clading	N+ $Al_xGa_{1-x}As(x = 0.05 - 0.45)$	1.05
5. Buffer	N+ GaAs	0.5

2. Device structure and fabrication

The laser diode device was prepared by metal–organic chemical vapor deposition. The structure of the wafer is shown in Table 1. The quantum well of the DFB laser is formed by the InGaAs/AlGaAs sandwich layers, and the average peak wavelength of PL spectrum is 891.9 nm.

Fig. 1 shows a schematic diagram of the device structure. The surface isolation grooves can be seen under a scanning electron microscope, as illustrated in Fig. 1(a). The periodic electrode windows were on the top of the mesas, There were grooves between every two mesas, This structure formed periodic electrodes. Fig. 1(b) shows how the currents were injected into the device from the electrode windows. The structure of the p-electrode leads to the gain differences in the active region.

The device was prepared in four steps. First, we patterned the periodic isolation grooves with a period of 6 μm ($\Lambda = 6$ μm) by i-line lithography and etched 500 nm by the inductively coupled plasma method. Second, we patterned the 4 μm wide ridge waveguide and etched 1000 nm. Third, we patterned the 1 μm periodic electrode windows on the mesas to create periodic current injection channels. There was a 300 nm silicon oxide layer on the surface except for the electrode windows. Finally, 500 nm metal was deposited on the surface by magnetron sputtering.

We wire-bonded a 1 mm long laser diode, with its p-side down on the heat sinks and tuned the temperature by a thermoelectric cooler (TEC) [28,29]. The periodic electrode windows led to a gain contrast in the active region and resulted in a gain-coupled mechanism.

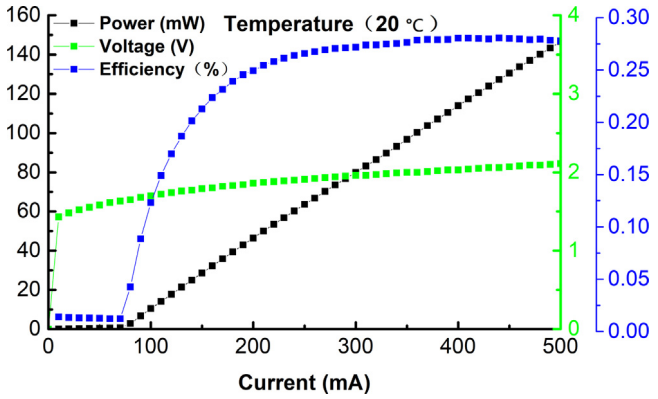

Fig. 2. CW power-voltage-current characteristics and electro-optical efficiency profiles at 20 °C.

3. Results and discussion

A continuous-wave (CW) test was carried out at 20 °C. The power-voltage-current (P-I-V) and electro-optical efficiency curves of the device are shown in Fig. 2 (measured by Newport PMKIT-15-01). The data in Fig. 2 were obtained by measuring one facet of the device, and the conversion efficiency was calculated by doubling the tested output power of one facet, so as to obtain the total value. The device had a threshold current of 85 mA. The output power reached 145.3 mW/facet at 500 mA. It is obvious that the output power increased linearly from 85 to 500 mA. The slope efficiency was 0.34 W/A. Fig. 2 shows a rapid increase in the conversion efficiency in the range of 100–200 mA, caused by more electron–hole pairs recombining when the injected currents increase. Thereafter, it increases slowly from 200 to 400 mA. When the injected current was 400 mA, the conversion efficiency was over 28%. The efficiency decreased when the injected currents exceeded 400 mA. There was damage to the device once the injected currents exceeded 400 mA after repeated tests, because of the accumulated thermal effect [30]. Therefore, the injected currents should remain below 400 mA.

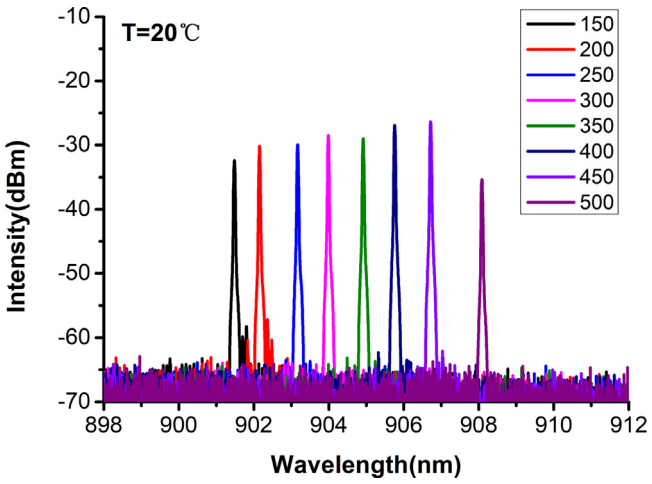

Fig. 3. CW spectrum characteristics of the tunable DFB laser with different injection current at 20 °C.

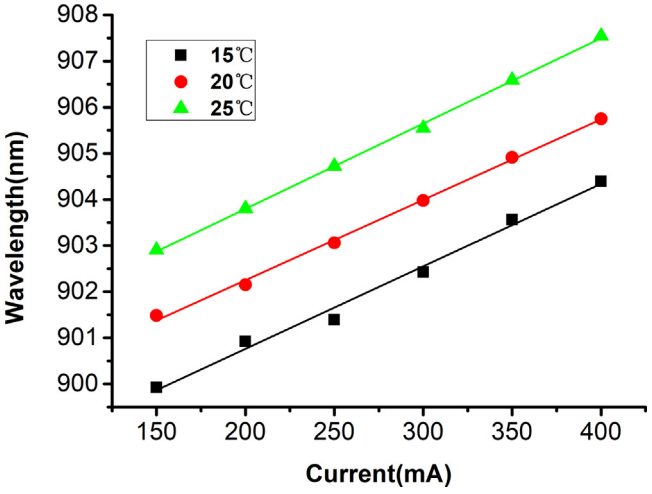

Fig. 4. Center wavelength of the tunable DFB laser diode with different current and temperature.

The spectra at 20 °C are clearly shown in Fig. 3. The spectra were measured directly by coupling the laser using a 10 μm core diameter fiber-linking YOKOGAWA AQ6370C optical spectrum analyzer. The SMSRs were less than 30 dB, When the injected currents were less than 200 mA. the SMSRs were over 33 dB and increased steadily with increasing currents when the injected currents exceeded 250 mA. This phenomenon is due to the variation of quantum well working state under different current injection conditions and material linewidth enhancement factor. Compared with the spectral characteristics between 400 and 500 mA, the spectrum was stable at 400 mA after many repeated experiments. The performance was temporarily stable at 450 mA, and then, the spectrum deteriorated rapidly. The SMSR decreased rapidly at the same time. The spectrum at 500 mA shows the deterioration. The current of 400 mA is over 4 times that of the threshold. Considering the narrow-stripe ridge waveguide structure, the output power density needs to be controlled within a reasonable range to prevent device damage. Once again, the injected currents should be controlled below 400 mA to achieve desirable performance and avoid irreversible damage [31].

The working wavelengths of the device versus different operating temperatures and currents can be fitted to linear curves, as illustrated in Fig. 4. The device could be tuned from 899.9 to 903.8 nm at 15 °C, from 901.4 to 905.2 nm at 20 °C, and from 902.8 to 907.7 nm at

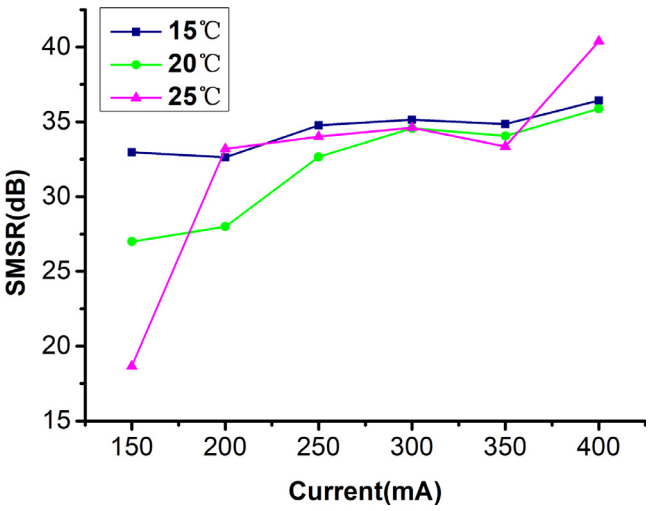

Fig. 5. SMSR of the tunable DFB laser diode with different currents and temperatures.

25 °C. The slope efficiencies of all the three curves were almost the same. At a given temperature, the wavelengths increased uniformly as the injected currents increased. The gain spectrum of the gain-coupled DFB laser is wider than the index-coupled DFB laser and The gain spectrum will be changing with the fluctuation of the injection current. The single longitudinal mode is achieved by the isolation grooves. Fig. 4 shows that the points are in straight lines and the points are uniformly distributed in the vertical direction, When the injected current is fixed. This means that the redshift at a given injected current was stable from 15 °C to 20 °C and 25 °C. The expected tunable phenomenon was realized. Thus, it was demonstrated that the working wavelength of DFB laser diode could be tuned from 899.9 to 907.7 nm under changing temperature and injected currents. A range of 7.8 nm was achieved with only one pair of P and N electrodes.

Fig. 5 shows the fluctuation of SMSRs at different temperatures. Overall, it was observed that the SMSRs gradually increase with increasing injected currents at any specified temperature and are always over 32 dB at 15 °C. Compared to 20 and 25 °C, the inhibition of SMSRs was more stable when the temperature was lower. The SMSRs decreased with the rise in temperature at 150 mA (Fig. 5). However, the SMSRs at 20 and 25 °C tended to be stable with the increasing injected currents. The SMSR is over 37 dB when the injected current is 400 mA at 25 °C. The increasing injected currents led to an increase in the concentration of the injection carriers. The carrier concentration and the temperature variation resulted in a gradient in the diffusion and recombination rate variations. The diffusion length of the carriers became larger and the gain coupled effect changed because of the periodic electrode channels. According to the Einstein relation, the diffusion coefficient is proportional to the temperature inside the device. In the dynamic process of the device, both the heat generated inside the device and the cooling of TEC affected the performance of the device. Therefore, the fluctuations in the SMSRs were affected by many factors.

Fig. 6 shows the 3 dB linewidth of the device at 20 °C, when the injected current was 300 mA. The linewidth was measured by coupling the collimated laser to the Fabry–Perot interferometer (Thorlabs, SA200-8B), which has a resolution of 67 MHz and free spectral range of 10 GHz. The linewidth is calculated as $\Delta\nu = (t_{FWHM}/\Delta t) * \nu_0$ where the t_{FWHM} is the full width at half maximum(FWHM) of the scanned spectrum,Δt is the interval between the scanned spectrum, andν_0 is the free spectral range. The 3 dB linewidth was about 920 MHz. The variation in the injected currents results in a change in the real and imaginary parts of the refractive index of the device. The increase in the injected currents enhances spontaneous radiation and broadens the linewidth. However, such a device can still meet the requirements in

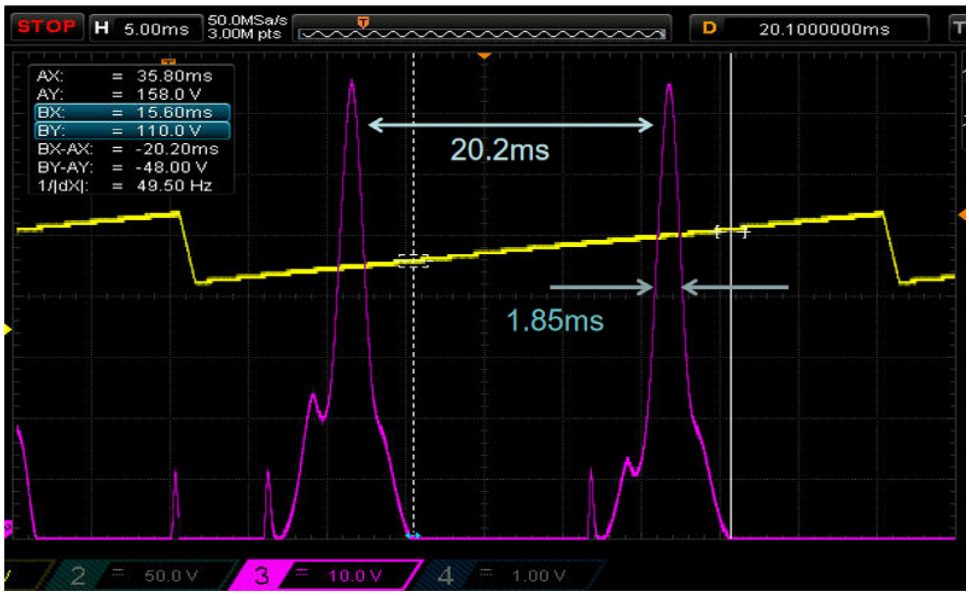

Fig. 6. Linewidth image of the tunable DFB laser working at 300 mA.

many application areas. Compared to the surface gratings lasers and vertical-cavity surface-emitting lasers, they are of the same order of magnitude [32,33]. Furthermore, the linewidth could be compressed and narrowed by coating films and adding an external filter.

4. Conclusion

We have presented a 905 nm tunable DFB laser diode with periodic surface isolation grooves. The method of fabrication is cost-effective and does not introduce regrowth technology and the structure is suitable for integration. The uncoated device reached a CW power of 145.3 mW/facet. The SMSR of the device was over 37 dB. We demonstrated that the device realizes a good single longitudinal mode output performance. We achieved the expected tunability within a range of 7.8 nm by controlling the injected currents and operating temperature. The 3 dB linewidth of the uncoated device was 920 MHz. Hence, this DFB laser can meet the requirements of many applications, e.g., LiDAR. Future work will be concentrated on developing a tunable laser array around 905 nm.

Declaration of competing interest

The authors declare that they have no known competing financial interests or personal relationships that could have appeared to influence the work reported in this paper.

Acknowledgments

This work is supported by National Science and Technology Major Project of China (2018YFB2200300); Frontier Science Key Program of the President of the Chinese Academy of Sciences (QYZDY-SSW-JSC006); National Natural Science Foundation of China (NSFC) (11874353, 61935009, 61934003, 61604151, 61674148, 61904179, 61727822, 11604328, 61805236); Dawn Talent Training Program of CIOMP, China.

References

[1] Y. He, H. An, J. Cai, et al., 808 nm broad area DFB laser for solid-state laser pumping application, Electron. Lett. 45 (3) (2009) 163–164.
[2] J.C. Yong, L. Thevenaz, B.Y. Kim, Brillouin fiber laser pumped by a DFB laser diode, J. Lightwave Technol. 21 (2) (2003) 546–554.
[3] Z. Zhou, B. Yin, J. Michel, On-chip light sources for silicon photonics, Light Sci. Appl. 4 (11) (2015) e358.
[4] Biasco Simone, Harvey, et al., Frequency-tunable continuous-wave random lasers at terahertz frequencies, Light Sci. Appl. (2019).
[5] S. Cakmakyapan, P.K. Lu, A. Navabi, et al., Gold-patched graphene nano-stripes for high-responsivity and ultrafast photodetection from the visible to infrared regime, Light Sci. Appl. 7 (2018) 20, http://dx.doi.org/10.1038/s41377-018-0020-2.
[6] T. Tanabe, S. Ragam, Y. Oyama, Continuous wave terahertz wave spectrometer based on diode laser pumping: Potential applications in high resolution spectroscopy, Rev. Sci. Instrum. 80 (11) (2009) 113105.
[7] X. Zhu, C. Zhang, J. Qiu, et al., Research on characteristics of GaAs PCSS triggered by 905 nm laser diode array, in: 2016 IEEE International Power Modulator and High Voltage Conference, IPMHVC, IEEE, 2016.
[8] L. Zeng, G. Liu, D. Yang, et al., Portable optical-resolution photoacoustic microscopy with a pulsed laser diode excitation, Appl. Phys. Lett. 102 (5) (2013) 053704.
[9] L. Leggio, D.C. Gallego, S.B. Gawali, et al., Optoacoustic response from graphene-based solutions embedded in optical phantoms by using 905-nm high-power diode-laser assemblies, in: Spie Photonics West, Photons Plus Ultrasound: Imaging & Sensing, 2016.
[10] J. Wojtanowski, M. Zygmunt, M. Kaszczuk, et al., Comparison of 905 nm and 1550 nm semiconductor laser rangefinders' performance deterioration due to adverse environmental conditions, Opto-Electron. Rev. 22 (3) (2014) 183–190.
[11] D.D. Macik, T.E. Bravo, S.M. Pentecost, et al., Optimization of electro-optic phase shifters for integrated optical phased arrays, in: Spie Defense Security. Society of Photo-Optical Instrumentation Engineers (SPIE) Conference Series, 2017.
[12] Y.P. Chang, C.N. Liu, Z. Pei, S.M. Lee, Y.K. Lai, P. Han, et al., New scheme of LiDAR-embedded smart laser headlight for autonomous vehicles, Opt. Express 27 (20) (2019) A1481–A1489.
[13] Andrea Knigge, Andreas Klehr, Hans Wenzel, et al., Wavelength-stabilized high-pulse-power laser diodes for automotive LiDAR, Adv. Sci. News 215 (2018).
[14] S. Lourdudoss, A. Ovtchinnikov, Entirely aluminum free 905-nm wavelength buried heterostructure laser by reactive ion etching and semi-insulating GaInP:Fe regrowth, IEEE Trans. Electron Devices 44 (2) (1997) 339–340.
[15] V.V. Wong, A. Schoenfelder, S. O'Brien, et al., High-brightness αDFB arrays at 915 nm and 1.06 μm, Cleo, 1999, pp. 46–47.
[16] P.D. Carro, A. Camposeo, R. Stabile, et al., Near-infrared imprinted distributed feedback lasers, Appl. Phys. Lett. 89 (2006).
[17] M. Al-Mumin, W. Mao, Y. Li, G. Li, 40 ghz millimetre-wave link based on two-section gain-coupled dfb lasers, Electron. Lett. 37 (14) 915-0.
[18] F. Gao, L. Qin, Y. Chen, et al., Study of gain-coupled distributed feedback laser based on high order surface gain-coupled gratings, Opt. Commun. 410 (2018) 936–940.
[19] Yuxin Lei, Yongyi Chen, Feng Gao, Dezheng Ma, Peng Jia, Hao Wu, Chunkao Ruan, Lei Liang, Chao Chen, Jun Zhang, Li Qin, Yongqiang Ning, Lijun Wang, 996 nm high-power single-longitudinal-mode tapered gain-coupled distributed feedback laser diodes, Appl. Opt. 58 (2019) 6426–6432.
[20] F. Gao, L. Qin, Y. Chen, et al., Two-segment gain-coupled distributed feedback laser, IEEE Photonics J. PP (99) (2018) 1.

[21] F.H. Peters, D.T. Cassidy, Model of the spectral output of gain-guided and index-guided semiconductor diode lasers, J. Opt. Soc. Amer. B 8 (1) (1991) 99–105.
[22] B. Corbett, D. Mcdonald, Single longitudinal mode ridge waveguide 1.3 μm Fabry-Perot laser by modal perturbation, Electron. Lett. 31 (25) (1995) 2181–2182.
[23] J. Patchell, D. Jones, B. Kelly, J. O'Gorman, Specifying the wavelength and temperature tuning range of a Fabry–Perot laser containing refractive index perturbations, in: Proc. SPIE, Vol. 5825, 2005, pp. 1–13.
[24] S. O'Brien, E.P. O'Reilly, Theory of improved spectral purity in index patterned Fabry–Perot lasers, Appl. Phys. Lett. 86 (2005) 201101-1–201101-3.
[25] B. Kelly, R. Phelan, D. Jones, C. Herbert, J. O'Carroll, M. Rensing, J. Wendelboe, C.B. Watts, A. Kaszubowska-Anandarajah, P. Perry, C. Guignard, L.P. Barry, J. O'Gorman, Discrete mode laser diodes with very narrow linewidth emission, Electron. Lett. 43 (2007) 1282–1284.
[26] R. Phelan, W.-H. Guo, Q.Y. Lu, D. Byrne, B. Roycroft, P. Lambkin, B. Corbett, F. Smyth, L.P. Barry, J. Patchell, B. Kelly, J. O'Gorman, J.F. Donegan, A novel two-section tunable discrete mode Fabry–Pérot laser exhibiting nanosecond wavelength switching, IEEE J. Quantum Electron. 44 (4) (2008) 331–337.
[27] W.H. Guo, D. Byrne, R. Phelan, et al., Characterization of reflective defects in Fabry–Pérot laser diodes through the power transmission spectrum, IEEE J. Quantum Electron. 43 (2007) 350–357.
[28] H. Chen, Y. Chen, F. Gao, et al., Narrow-strip 640 nm Gaub-coupled distributed feedback laser based on periodic anodes fabricated by I-line lithography, IEEE Photon. J. 11 (3) 1–9.
[29] Y.Y. Chen, P. Jia, J. Zhang, et al., Gain-coupled distributed feedback laser based on periodic surface anode canals, Appl. Opt. 54 (30) (2015) 8863–8866.
[30] K. Shima, H. Watanabe, H. Yonetani, et al., Aging characteristics of InGaAsP DFB laser, in: Optical Fiber Communication Conference, 1988.
[31] D. Livshits, I. Kochnev, V. Lantratov, et al., Improved catastrophic optical mirror damage level in InGaAs/AlGaAs laser diodes, Electron. Lett. 36 (22) (2000) 1848–1849.
[32] S.K. Pavan, J. Lavrencik, S.E. Ralph, Experimental demonstration of 51.56 Gbit/s PAM-4 at 905 nm and impact of level dependent RIN, 2014.
[33] H. Wenzel, J. Fricke, J. Decker, et al., High-power distributed feedback lasers with surface gratings: Theory and experiment, IEEE J. Sel. Top. Quantum Electron. 21 (6) (2015).